

First principles study on small $ZrAl_n$ and $HfAl_n$ clusters: structural, stability, electronic states and CO_2 adsorption

Hardik L. Kagdada¹, Shweta D. Dabhi², Venu Mankad², Satyam M. Shinde³, Prafulla K. Jha^{1*}

1. Department of Physics, Faculty of science, The M. S. University of baroda. Vadodara – 390002, INDIA
 2. Department of Physics, M. K. Bhavnagar University, Bhavnagar – 364001, INDIA
 3. School of Technology, Pandit Deendayal Petroleum University, Gandhinagar – 382007, INDIA
- *prafullaj@yahoo.com

Abstract

We report a first principles study based on density functional theory on the structural and electronic properties of transition metal Zr and Hf doped small aluminum clusters with 1 to 7 aluminum atoms. We have used B3PW91/LANL2DZ basis set in Gaussian 09 package. The stability analysis reveals that the $ZrAl_4$ and $HfAl_4$ structures with C_{2v} symmetry and square pyramid geometry are lowest energy structures. The most stable structures in $ZrAl_5$ and $HfAl_5$ are distorted tetrahedron type structure with symmetry C_1 . The binding energies per atom for transition metal doped Al_n clusters increases with the cluster size, while the second order difference in total energy show oscillatory behavior with even and odd cluster size. The HOMO – LUMO gap for $ZrAl_n$ is larger than the $HfAl_n$ clusters except for $n = 1$ and 3. The $HfAl_6$ has more tendency to accept or give away electrons. The negative charge exists on Zr and Hf indicating that the electron transfers from Al atom to transition metal, Zr and Hf. The thermodynamical analysis suggest that the $HfAl_6$ cluster has highest exothermicity compared to not only all considered Al clusters but also other transition metal doped Al clusters reported in J. Phys. Chem. C, 120, 10027 (2016).

Keywords: clusters; electronic states; stability; CO_2 adsorption

1. Introduction

In recent years great deal of attention is devoted to clusters due to their fundamental concept of electronic and geometrical stability and potential application in variety of fields such as catalytic activities, hydrogen storage¹⁻⁴, formation of metallic glasses^{5,6} and most importantly alternate building blocks of materials in the form of super atoms⁷. Among the variety of clusters, binary metallic clusters have much attention due to their wide range of tailoring properties about its size, shape and chemical composition⁸⁻¹². Furthermore, binary metallic clusters are used to control the synthesis and chirality of the single walled carbon nano tubes (SWCNT)¹³. As a typical example of atomic and doped atomic clusters, the aluminum and transition metal (TM) doped aluminum clusters respectively have been the subject of many investigations¹⁴⁻²⁹. The display of large local magnetic moments by the transition metal doped aluminum clusters is one of the main reason for their increasingly focused studies²⁹. The existence of large local magnetic moments is attributed to the interaction of d electron with the nearly free electron gas when the TM element is present in sp metal host or surfaces. Wang et. Al²⁹ studied the structural, electronic and magnetic properties of MAI_n ($M = Cr, Mn, Fe, Co, Ni; n = 1 - 7, 12$) clusters using density functional theory (DFT) by treating the exchange-correlation interaction with generalized gradient approximation (GGA). While they found non-degenerate and delocalized HOMO and LUMO states, the computed total magnetic moment oscillate with the cluster size. Very recently, the influence of spin on the properties of small sized transition metal doped aluminum clusters using DFT is reported⁷. Their low spin doped aluminum clusters show the odd even oscillation in various calculated properties in the line of jellium shell structures in contrast to the high spin case which show smooth variation in the properties. However in comparison, Zr and Hf based transition metal doped Al clusters have not been studied systematically and lacks the information on stability, structures, electronic, heat of absorption on the cluster surface. Zr and Hf transition metal elements possess many interesting properties like high coercivity and low absorption cross section for neutrons.

There exist few studies based on Zr-Al compounds using DFT calculations³⁰⁻³⁵. Wang et. al³⁰. studied the phase stability, mechanical and thermodynamical properties of Zr-Al binary substitutional alloys and found that the $ZrAl_2$ is most stable with excellent mechanical properties, while $ZrAl_3$ possesses better thermal conductivity and higher melting temperature³⁰. Arikan³¹ has

reported the elastic, electronic and phonon properties of Zr_3Al compound. A stability and thermodynamic property of Zr_2Al under high pressure is reported using DFT method within GGA for exchange and correlation³⁵. De Souza³² et. al. performed a basin-hopping Monte Carlo investigation within the embedded-atom method for the structural and energetic properties of bimetallic $ZrCu$ and $ZrAl$ nanoclusters with 55 and 561 atoms and found that unary systems adopt the well-known compact icosahedron (ICO) structure. However, the ICO structure changes to the nearly spherical shape due to strong minimization of the surface energy when both chemical species change towards a more balanced compositions. DFT study of structural and electronic properties of $Zr_nAl^{\pm m}$ ($n = 1 - 7$, $m = 0, 1$) clusters shows that all stable structures are three dimensional for $n > 3$ and binding increases as n increases for all considered $Zr_nAl^{\pm m}$ ³³.

In recent time the sequestration of the CO_2 emitted from industrial manufacturing plants is one of the most pressing issues in the environmental protection. An ideal CO_2 sequestration material should have large surface areas and strong adsorption sites. Many CO_2 adsorbents including metal organic frameworks (MOFs), carbon and silicon carbide and boron rich boron nitride have limitations in terms of interactions^{36 - 40}. Clusters have been found good not only to absorb the CO_2 but also H_2 , O_2 , and N_2 . Sengupta et. al.⁷ have studied the CO_2 absorption over transition metal series from Sc to Zn doped aluminum clusters (Al_5 and Al_7) and found that the starting element of series Sc and Ti doped Al clusters are good absorber. Therefore, it would be of interest to see the absorption capability of non-magnetic and closer to Sc and Ti elements, Zr and Hf doped aluminum clusters.

In the present paper, on the basis of results of first principles calculations using theories of plane waves and localized atomic orbitals we report relative stability, binding energy and electronic properties of Zr and Hf doped Al clusters. Furthermore, we report that the Zr and Hf doped Al clusters can capture CO_2 more strongly than the reported other transition metal doped Al clusters. The structures of optimized clusters and CO_2 clusters conformers are found to be consistent with available similar CO_2 cluster conformers.

2. Computational method

In the present study all the calculations were performed using density functional theory simulation on $TmAl_n$ clusters using GAUSSIAN 09 package⁴¹. The Becke's three parameter (B3)

and Perdew and Wang (PW91) GGA functional together called the B3PW91 were used for the exchange and correlation respectively along with Los Alamos set of double-zeta type (LANL2DZ)⁴²⁻⁴⁴ basis set to derive a complete geometrical optimization of transition metal Zr and Hf doped Al_n (n = 1 – 7) clusters. The accurate determination of ground state geometry of cluster is required in the chemistry of clusters. Initially different arrangements of isomers of clusters are taken for each cluster to obtain the ground state conformers. After optimization of all these isomers the energetically minimum structure is taken as ground state geometry for each cluster. Binding energy between transition metal and Al_n clusters is calculated using the following formula

$$E_b(n) = \frac{[nE(Al)+nE(Tm)-E(TmAl_n)]}{n+1} \quad (1)$$

where E(Al) and E(Tm) is the total energy of one atom of Al and transition metal (Zr, Hf) respectively and E(TmAl_n) is the total energy of transition metal doped Al_n cluster. The relative stability of the cluster is defined by the second order difference in the total energy which was calculated by the following formula

$$\Delta^2 E = E(TmAl_{n-1}) + E(TmAl_{n+1}) - 2E(TmAl_n) \quad (2)$$

Chemical hardness defines the tendency to gain or give the electrons is calculated using the following formula^{45, 46}

$$\eta = \frac{I.E.-E.A.}{2} \quad (3)$$

where I.E. = Ionization Energy and E.A. = Electron Affinity. The difference in energy of neutral cluster and cation of that cluster are taken to evaluate the ionization energy and the difference in energy of neutral cluster and anion of that cluster are taken to evaluate the electron affinity. The behavior of charge transfer between transition metal and Al cluster, natural electronic configuration are calculated using natural bond analysis (NBO) which is implemented in Gaussian 09 package^{47, 48}.

3. Result and Discussion

3.1 Structural Geometry:

For calculation of any ground state properties one needs to optimize the structures and obtain the equilibrium geometrical structures. Figs. 1 and 2 present the fully optimized ground state and low lying structures of transition metal doped Al_n clusters (TmAl_n ; TM = Zr and Hf, $n = 1$ to 7). The point group and the multiplicity are listed in Table – I. The Table – I also lists the binding energy, second order difference in total energy and ionization energy for ZrAl_n and HfAl_n clusters. Relatively lowest energy structure is found for $n = 2$ i.e. for ZrAl_2 and HfAl_2 with the point group symmetry C_s and C_{2v} for ZrAl_2 and HfAl_2 respectively. They have a shape of isosceles triangle with angle 58.164° for Al-Zr-Al and 59.585° for Al-Hf-Al. For $n = 3$ minimum energy structure is found for C_s symmetry while other ZrAl_3 and HfAl_3 structures are 2.31 eV and 2.66 eV higher in energy, respectively. ZrAl_4 and HfAl_4 structures with C_{2v} symmetry and square pyramid geometry are lowest energy structures while others have distorted tetrahedral C_1 symmetry with higher energy. The most stable structure in ZrAl_5 and HfAl_5 are distorted tetrahedron type structure with symmetry C_1 while other structures of ZrAl_5 and HfAl_5 with C_{2v} symmetry are 1.74 eV and 1.85 eV higher in energy. TmAl_6 structures have both C_{4v} and C_{2v} type symmetry. The C_{4v} type structures have 2.13 eV and 1.24 eV higher energy than that of C_{2v} type structure for ZrAl_6 and HfAl_6 respectively. The structures with pentagonal bi pyramid C_{2v} are ground state structures for TmAl_6 which is similar to the FeAl_6 clusters²⁹. The ground state isomers of ZrAl_7 and HfAl_7 are to be found by capping of Al atom on the pentagonal bipyramid structures of TmAl_6 and having symmetry C_{2v} . All calculations are performed for the most energetically stable structures.

3.2 Stability

For the analysis of relative stability of TmAl_n clusters we have calculated binding energy per atom $E_b(n)$ and 2nd order difference in the total energy Δ^2E of the clusters using the equations (1) and (2) respectively presented in section 2. The second order difference in the total energy is the quantity which defines the relative stability of the clusters⁴⁹. The calculated values of $E_b(n)$ and Δ^2E for ground state structures are listed in Table – I. The binding energy per atom increases with the increasing in cluster size as can be seen from Fig. 3(a). Table – I and Fig. 3(b) show that

the Δ^2E behaves oscillatory with cluster size. The fluctuation behavior of Δ^2E is more for HfAl_n than ZrAl_n . However, we observe that the Δ^2E is higher for clusters of even number, which is similar to the clusters of $\text{Zr}_n\text{Al}^{\pm m}$ ³³. The maximum peak observed at $n = 4$ for HfAl_4 suggest that HfAl_4 is the most stable cluster than its nearest neighbors ($n = 3, 5$). This can also be seen from the Fig. 3(a) that the HfAl_4 has highest binding energy. As for $n = 6$, ZrAl_n is concerned that the $n = 6$ is most stable, which can also be seen from the Fig. 3(a) where binding energy is highest for ZrAl_6 . All the calculations presented in the following sections are performed for the most energetically stable structures.

3.3 Electronic properties

Electronic properties of clusters can be analyzed through Highest Occupied Molecular Orbital (HOMO) and Lowest Unoccupied Molecular Orbital (LUMO) orbitals. HOMO – LUMO orbital play an important role in the process of chemical reactions hence, its analysis can help in studying the chemical stability of the clusters. The molecule can be easily excited if the gap is smaller. Fig. 4(a) shows the HOMO – LUMO gap (G_{HL}) for TmAl_n clusters as a function of cluster size n . The HOMO – LUMO gap for ZrAl_n is larger than the HfAl_n clusters except for $n = 1$ and 3 . Maximum and minimum gap is found for HfAl and HfAl_4 respectively with the value of 2.214 eV and 0.159 eV which indicates that the HfAl cluster has relatively higher chemical stability and HfAl_4 is more inert cluster than others. Chemical hardness (η) as a function of cluster size (n) is presented in Fig. 4(b) and listed in Table – II. Chemical hardness is the measure of the cluster to accept or give away electrons i.e. bigger η suggest the smaller tendency and smaller η suggest the larger tendency for accepting or give away the electrons⁵⁰. Table – II shows that the HfAl_6 has minimum η with 1.825 eV indicating that the HfAl_6 has more tendency to accept or give away electrons.

3.4 NBO analysis

The natural electronic configuration and charge transfer between considered transition metals and Al cluster can be studied by natural bond analysis (NBO). The natural electronic configuration and atomic charge on each atom in ZrAl_n and HfAl_n cluster presented in supplementary Table – I. The valance electron orbit for Zr, Hf and Al is $4d^2 5s^2$, $5d^2 6s^2$ and $3s^2 3p^1$ respectively. The range of electrons in $3s$ orbital of Al in ZrAl_n is from 1.28 to 1.84 and that

in HfAl_n within 1.21 to 1.81, which shows that the 3s orbital of Al loses the electrons. While for 3p orbit of Al gains the electrons as the occupation of electrons in 3p orbital of Al in ZrAl_n within 1.07 to 1.97 and that for the HfAl_n has range of 1.11 to 1.93. The contribution of 4p orbitals of Al in both type of clusters can be neglected as the electrons in this orbit is in the range of 0.01 – 0.02. This shows that the hybridization of Al in Zr and Hf doped Al_n is sp hybridization. The electrons in 4d orbitals of Zr is between 2.61 and 4.14, while for electron in 5s orbital of Zr within 0.47 to 1.32. This indicates that the 5s orbital of ZrAl_n clusters loses the electrons, while 4d orbitals occupied more electrons. The occupation nature of electrons is similar for HfAl_n clusters as 5d orbital gain the electrons while 6s orbit loses the electrons. It is observed from supplementary Table – I that occupation of electrons in 5p orbital of Zr is in between 0.10 and 0.62, while for HfAl_n within 0.21 to 0.75. This occupation shows that the Zr and Hf has spd hybridization in Al_n clusters. The natural electronic configuration indicates that the loss of electrons in 3s orbitals of Al is more than the gain of electrons in 3p orbital. However, the loss of electrons in 5s orbitals of Zr is less than the occupied electrons in 4d orbital of Zr in ZrAl_n clusters and similar phenomena happens in HfAl_n . This indicates that the charge transfers from aluminum to Zr and Hf respectively in ZrAl_n and HfAl_n clusters and both Zr and Hf have negative charge as can be seen from Table – II.

3.5 Adsorption of CO_2 on TmAl_n Clusters

We have computed the thermodynamic data of the adsorption of CO_2 on the Hf and Zr doped Al_n ($n = 4 - 7$) clusters and compare them with the available data on other transition metal doped Al clusters⁷. The literature reveals that there are mainly two different configuration of bonding between CO_2 and TmAl_n clusters. One is series bonding i.e. the one O atom from CO_2 bind with the transition metal of cluster and other is the parallel bonding i.e. the one oxygen atom bind with transition metal and other oxygen atom bind with the one aluminum cluster. In the present calculation we take parallel configuration because Sengupta⁷ et. al. have reported that the series binding has low exothermicity of adsorption. Figs. 5 (a-h) show the optimized structures of transition metal Hf and Zr doped Al_n clusters with adsorption of CO_2 in parallel binding configuration. Thermochemical parameters (ΔE , ΔH and ΔG) are listed in Table – III which depicts that the HfAl_6 cluster has highest exothermicity compared to the other Hf and Zr doped Al_n clusters. It is interesting to note that the exothermicity for HfAl_6 is even higher than the Sc

and Ti doped aluminum clusters⁷. Furthermore, one can observe that in all cases the angle of CO₂ is changed and the bond length between CO₂ and cluster is increased as observed in the case of other transition metal doped Al_n clusters.

4. Conclusions

In summary we have performed the density functional theory calculations with the basis set of LANL2DZ of two transition metals (Zr and Hf) doped aluminum clusters. We report energetically stable geometries, electronic structure and relative stability of Zr/Hf Al_n (n = 1 – 7) clusters. All the calculations are performed for the most energetically stable structures. The Zr and Hf doped Al_n clusters favor 3D spatial structures at the smaller number of Al atoms compared to higher number of Al clusters. The natural electronic configuration analysis shows that the electron moves from Al_n clusters to transition metal Zr and Hf. We found that the binding energy of considered clusters is increasing with increase in cluster size. HfAl₄ is relatively stable structure. From the HOMO – LUMO analysis we found that the ZrAl is relatively chemically more active with HOMO – LUMO gap of 2.124 eV. HfAl₆ cluster has more tendencies to accept or give away the electrons and higher enthalpy difference as well as higher adsorption of CO₂.

5. Supplementary Materials

See supplementary material for the natural bond analysis (NBO). The natural electronic configuration and atomic charge on each atom in ZrAl_n and HfAl_n cluster is presented in supplementary Table – I.

Acknowledgements

Authors are thankful to the SERB and DST for providing computational facility through project and FIST programs respectively. SD thanks DST for INSPIRE fellowship while VM thanks SERB for young scientist award.

References

1. S. Yamazoe, K. Koyasu and T. Tsukuda, “Nonscalable Oxidation Catalysis of Gold Clusters,” *Acc. Chem. Res.*, **47** (3), 824 (2014).
2. X. Tang, D. Bum Mueller, A. Lim, J. Schneider, U. Heiz, G. Ganteför, D. H. Fairbrother and K. H. Bowen, “Catalytic Dehydration of 2-Propanol by Size-Selected $(\text{WO}_3)_n$ and $(\text{MoO}_3)_n$ Metal Oxide Clusters,” *J. Phys. Chem. C* **118**, 29278-29286 (2014).
3. Y. Y. Wu, S. Y. Xu, F. Q. Zhao and X. H. Ju, “Adsorption and Dissociation of H_2 on B_n and MgB_n ($n = 2-7$) Clusters: A DFT Investigation,” *J. Clust. Sci.*, **26**(3), 983 (2015).
4. M. Maatallah, M. Guo, D. Cherqaoui, A. Jarid and J. F. Liebman, “Aluminium clusters for molecular hydrogen storage and the corresponding alanes as fuel alternatives: A structural and energetic analysis,” *International Journal of Hydrogen Energy* **38**, 5758 (2013)
5. A. Kartouzian, “Cluster-assembled metallic glasses,” *kartouzian nanoscale research letters*, **8**, 339 (2013)
6. J. A. Reyes-Retana and G. G. Naumis, “*Ab initio* study of Si doping effects in Pd–Ni–P bulk metallic glass,” *Journal of Non-Crystalline Solids*, **409**, 49-53 (2015).
7. T. Sengupta, S. Das and S. Pal, “Transition Metal Doped Aluminum Clusters: An Account of Spin,” *J. Phys. Chem. C*, **120**, 10027–10040 (2016).
8. R. Ferrando, “Symmetry breaking and morphological instabilities in core-shell metallic nanoparticles,” *J. Phys.: Condens. Matter* **27**, 013003 (2015).
9. F. Pittaway, L. O. Paz-Borbon, R. L. Johnston, H. Arslan, R. Ferrando, C. Mottet, G. Barcaro and A. Fortunelli, “Theoretical Studies of Palladium–Gold Nanoclusters: Pd–Au Clusters with up to 50 Atoms,” *J. Phys. Chem. C* **113**, 9141-9152 (2009).
10. J. L. F. Da Silva, M. J. Piotrowski and F. Aguilera-Granja, “Hybrid density functional study of small Rh_n ($n=2-15$) clusters,” *Phys. Rev. B* **86**, 125430 (2012).
11. F. Chen and R. L. Johnston, “Energetic, Electronic, and Thermal Effects on Structural Properties of Ag–Au Nanoalloys,” *ACS Nano* **2**, 165 – 175 (2008).
12. M. J. Piotrowski, P. Piquini and J. L. F. Da Silva, “Platinum-Based Nanoalloys $\text{Pt}_5\text{TM}_{55-n}$ (TM = Co, Rh, Au): A Density Functional Theory Investigation,” *J. Phys. Chem. C* **116**, 18432 (2012)
13. W. Chiang and R. M. Sankaran, “Linking catalyst composition to chirality distributions of as-grown single-walled carbon nanotubes by tuning $\text{Ni}_x\text{Fe}_{1-x}$ nanoparticles,” *Nature Materials*, **8**, 882 - 886 (2009).
14. X. G. Gong and V. Kumar, “Electronic structure and relative stability of icosahedral Al–transition-metal clusters,” *Phys. Rev. B*, **50**, 17701 (1994).
15. X. Li and L. S. Wang, “Experimental search and characterization of icosahedral clusters: Al_{12}X^- ,” *Phys. Rev. B*, **65**, 153404 (2002).

16. B. D. Leskiw and A. W. Castleman, Jr., "The interplay between the electronic structure and reactivity of aluminum clusters: model systems as building blocks for cluster assembled materials," *Chem. Phys. Lett.*, **316**, 31 (2000).
17. B. Kiran, P. Jena, X. Li, A. Grubisic, S. T. Stokes, G. F. Ganteför, K. H. Bowen, R. Burgert and H. Schnöckel, "Magic Rule for Al_nH_m Magic Clusters," *Phys. Rev. Lett.*, **98**, 256802 (2008).
18. B. K. Rao and P. Jena, "Evolution of the electronic structure and properties of neutral and charged aluminium clusters: A comprehensive analysis," *J. Chem. Phys.*, **111**, 1890 (1999).
19. S. Baroni, S. Gironcoli, A. Corso and P. Giannozzi, "Phonons and related properties of extended systems from density-functional perturbation theory," *Rev. Mod. Phys.* **73**, 515 (2001).
20. R. B. Russel, "On the Zr-Hf system," *J. Appl. Phys.* **24**, 232 (1953).
21. M. Potzschke and K. Schubert, "Towards the Synthesis of Several T_4-B_3 Homologous and Quasi-Homologous Systems. II The Systems Ti-Al, Zr-Al, Hf-Al, Mo-Al and Several Ternary Systems," *Z. Metallkde.*, **53**, 548-561 (1962).
22. H. M. Otte, W. G. Montague and D. O. Welch, "X-Ray Diffractometer Determination of the Thermal Expansion Coefficient of Aluminum near Room Temperature," *J. Appl. Phys.*, **34**, 3149 (1963).
23. F. D. Murnaghan, "The Compressibility of Media under Extreme Pressures," *Proc Natl AcadSci (U S A)*. **30**(9) 244–247 (1944).
24. P. K. Jha, "Phonon spectra and vibrational mode instability of $MgCNi_3$," *Phys. Rev. B*. **72**, 214502 (2005).
25. P.K. Jha and S.P. Sanyal, "A lattice dynamical study of the role of pressure on Raman modes in high- T_C $HgBa_2CuO_4$," *Physica C.*, **261**, 259-262 (1996).
26. P.K. Jha and S.P. Sanyal, "Phonon spectrum and lattice specific heat of the $HgBa_2CuO_4$ high-temperature superconductor," *Physica C.*, **271** 6-10 (1996).
27. P.K. Jha and S.P. Sanyal, "Lattice vibrations in Yb-pnictide compounds" *Phys. Rev. B.*, **52**, 15898 (1995).
28. C.Lee and X.Gonze, "*Ab initio* calculation of the thermodynamic properties and atomic temperature factors of SiO_2 α -quartz and stishovite," *Phys. Rev. B.*, **51**, 8610-8611 (1995).
29. M. Wang, X. Huang, Z. Du and Y. Li, "Structural, electronic, and magnetic properties of a series of aluminium clusters doped with various transition metals," *Chemical Physics Letters*, **480**, 258–264 (2009).
30. L. Wang, S. Hou, and D. Liang, "First-principles investigations on the phase stability, elastic and thermodynamic properties of Zr–Al alloys," *Int. J. Mod. Phys. C*, **26** (12) 1550143 (2015).

31. N. Arıkan, "The first-principles study on Zr₃Al and Sc₃Al in Ll₂ structure," *Journal of Physics and Chemistry of Solids*, **74**, 794 – 798 (2013).
32. D. G. De Souza, H. M. Cezar, G. G. Rondina, M. F. de Oliveira and J. L. F. Da Silva, "A basin-hopping Monte Carlo investigation of the structural and energetic properties of 55- and 561-atom bimetallic nanoclusters: the examples of the ZrCu, ZrAl, and CuAl systems," *J. Phys.: Condens. Matter*, **28**, 175302 (2016).
33. J. Yu, F. Zhao, S. Xu, L. Sun and X. Ju, "Density-Functional Study of Structural and Electronic Properties of the Zr_nAl^{±m} Clusters," *International Journal of Chemistry* **8**(4), 111 (2016).
34. P. V. S. Reddy, V. Kanchana, G. Vaitheeswaran, A. V. Ruban and N. E. Christensen, "Evidence for the antiferromagnetic ground state of Zr₂TiAl: a first principles study," *J. Phys.: Condens. Matter*, **29**, 265801 (2017).
35. X. L. Yuan, D. Q. Wei, Y. Cheng, Q. M. Zhang and Z. Z. Gong, "Thermodynamic properties of Zr₂Al under high pressure from first-principles calculations," *J. At. Mol. Sci.*, **3**(2) 160 – 170 (2012).
36. A. Pulido, M. R. Delgado, O. Bludsky, M. Rubes, P. Nachtigall, C. O. Arean, "Combined DFT/CC and spectroscopic studies on carbon dioxide on the H-FER," *Energy Environ. Sci.*, **2**, 1187 (2009).
37. J. Zhao, A. Buldum, J. Han, J. P. Lu, "Gas molecule adsorption in carbon nanotubes and nanotube bundles," *Nanotechnology*, **13**, 195 (2002).
38. L. Valenzano, B. Civalleri, S. Chavan, G. T. Palomino, C. O. Arean, S. J. Bordiga, "Computational and Experimental Studies on the Adsorption of CO, N₂, and CO₂ on Mg-MOF-74," *Phys. Chem. C*, **114**, 11185 (2010).
39. J. X. Zhao and Y. H. Ding, "Can Silicon Carbide Nanotubes Sense Carbon Dioxide?," *J. Chem. Theory Comput*, **5**, 1099 (2009).
40. H. Choi, Y. C. Park, Y. H. Kim and Y. S. Lee, "Ambient Carbon Dioxide Capture by Boron-Rich Boron Nitride Nanotube," *J. Am. Chem. Soc.*, **133**, 2084–2087 (2011).
41. M. J. Frisch, G. W. Trucks, H. B. Schlegel, G. E. Scuseria, M. A. Robb, J. R. Cheeseman, G. Scalmani, V. Barone, B. Mennucci, G. A. Petersson, H. Nakatsuji, M. Caricato, X. Li, H. P. Hratchian, A. F. Izmaylov, J. Bloino, G. Zheng, J. L. Sonnenberg, M. Hada, M. Ehara, K. Toyota, R. Fukuda, J. Hasegawa, M. Ishida, T. Nakajima, Y. Honda, O. Kitao, H. Nakai, T. Vreven, J. A. Montgomery, Jr., J. E. Peralta, F. Ogliaro, M. Bearpark, J. J. Heyd, E. Brothers, K. N. Kudin, V. N. Staroverov, T. Keith, R. Kobayashi, J. Normand, K. Raghavachari, A. Rendell, J. C. Burant, S. S. Iyengar, J. Tomasi, M. Cossi, N. Rega, J. M. Millam, M. Klene, J. E. Knox, J. B. Cross, V. Bakken, C. Adamo, J. Jaramillo, R. Gomperts, R. E. Stratmann, O. Yazyev, A. J. Austin, R. Cammi, C. Pomelli, J. W. Ochterski, R. L. Martin, K. Morokuma, V. G. Zakrzewski, G. A. Voth, P. Salvador, J. J. Dannenberg, S. Dapprich, A. D. Daniels, O. Farkas, J. B. Foresman, J. V. Ortiz, J. Cioslowski, and D. J. Fox, *Gaussian 09, Revision D.01*, Gaussian, Inc., Wallingford CT, (2013).

42. A. D. Becke, "Density functional thermochemistry. III. The role of exact exchange," *The Journal of Chemical Physics* **98**, 5648 (1993).
43. J. P. Perdew, K. Burke and Y. Wang, "Generalized gradient approximation for the exchange-correlation hole of a many-electron system," *Phys. Rev. B* **54**, 16533 (1996).
44. P. J. Hay and W. R. Wadt, "*Ab initio* effective core potentials for molecular calculations. Potentials for K to Au including the outermost core orbitals," *J. Chem. Phys.*, **82**, 299 – 310 (1985).
45. R. G. Pearson, "Chemical hardness and density functional theory," *J. Chem. Sci.*, **117**(5), 369–377 (2005).
46. Y. J. Suh, J. W. Chae, H. D. Jang and K. Cho, "Role of chemical hardness in the adsorption of hexavalent chromium species onto metal oxide nanoparticles," *Chem. Eng. J.*, **273**, 401-405 (2015).
47. J. E. Carpenter and F. Weinhold, "Analysis of the geometry of the hydroxymethyl radical by the "different hybrids for different spins" natural bond orbital procedure," *J. of Mol. Struct. (THEOCHEM)*, **169**, 41 – 49 (1988).
48. A. E. Reed, L. A. Curtiss, and F. Weinhold, "Intermolecular interactions from a natural bond orbital, donor-acceptor viewpoint," *Chem. Rev.*, **88**(6), 899–926 (1988).
49. J. Wang, Y. Liu, and Y. C. Li, "Au@Si_n: Growth behavior, stability and electronic structure," *Phys. Lett. A* **374**(27), 2736-2742 (2010).
50. R. G. Parr, and Z. X. Zhou, "Absolute hardness: unifying concept for identifying shells and subshells in nuclei, atoms, molecules, and metallic clusters," *Acc. Chem. Res.*, **26**, 256-258 (1993).

Figure caption

Figure – 1: Lowest energy and low lying energy structures of $ZrAl_n$, ($n = 1$ to 7). Here first digit denotes the number of aluminum and the characters (a, b, c) shows the structure label (lowest energy to highest energy structures.) Red color is for Zirconium and blue for the aluminum.

Figure – 2: Lowest energy and low lying energy structures of $HfAl_n$, $n = 1$ to 7 . Here first digit denotes the number of aluminum and the characters (a, b, c) shows the structure label (lowest energy to higher energy structures) Cyan color is for hafnium and blue color for the aluminum).

Figure – 3: (a) Binding energy and (b) second order difference in total energy for $ZrAl_n$ and $HfAl_n$ clusters.

Figure – 4: (a) HOMO-LUMO gap and (b) Chemical hardness for $ZrAl_n$ and $HfAl_n$ clusters.

Figure – 5: Ground structures of CO_2 doped $ZrAl_n$ (a, b, c, d), $HfAl_n$ (e, f, g, h), $n = 4 - 7$ and (i) CO_2 structure.

Figure – 6: Thermochemical data on absorption of CO_2 for (a) $ZrAl_n$ and (b) $HfAl_n$

Table caption

Table – I: Structural symmetry, binding energy and second order difference in total energy with ionization energy for the $ZrAl_n$ and $HfAl_n$ clusters.

Table – II: HOMO-LUMO gap, Atomic charge on Tm and chemical hardness for $ZrAl_n$ and $HfAl_n$.

Table – III: Thermochemical data (enthalpy and free energy difference) of adsorption of CO_2 on $ZrAl_n$ and $HfAl_n$ ($n = 4$ to 7).

Figure – 1

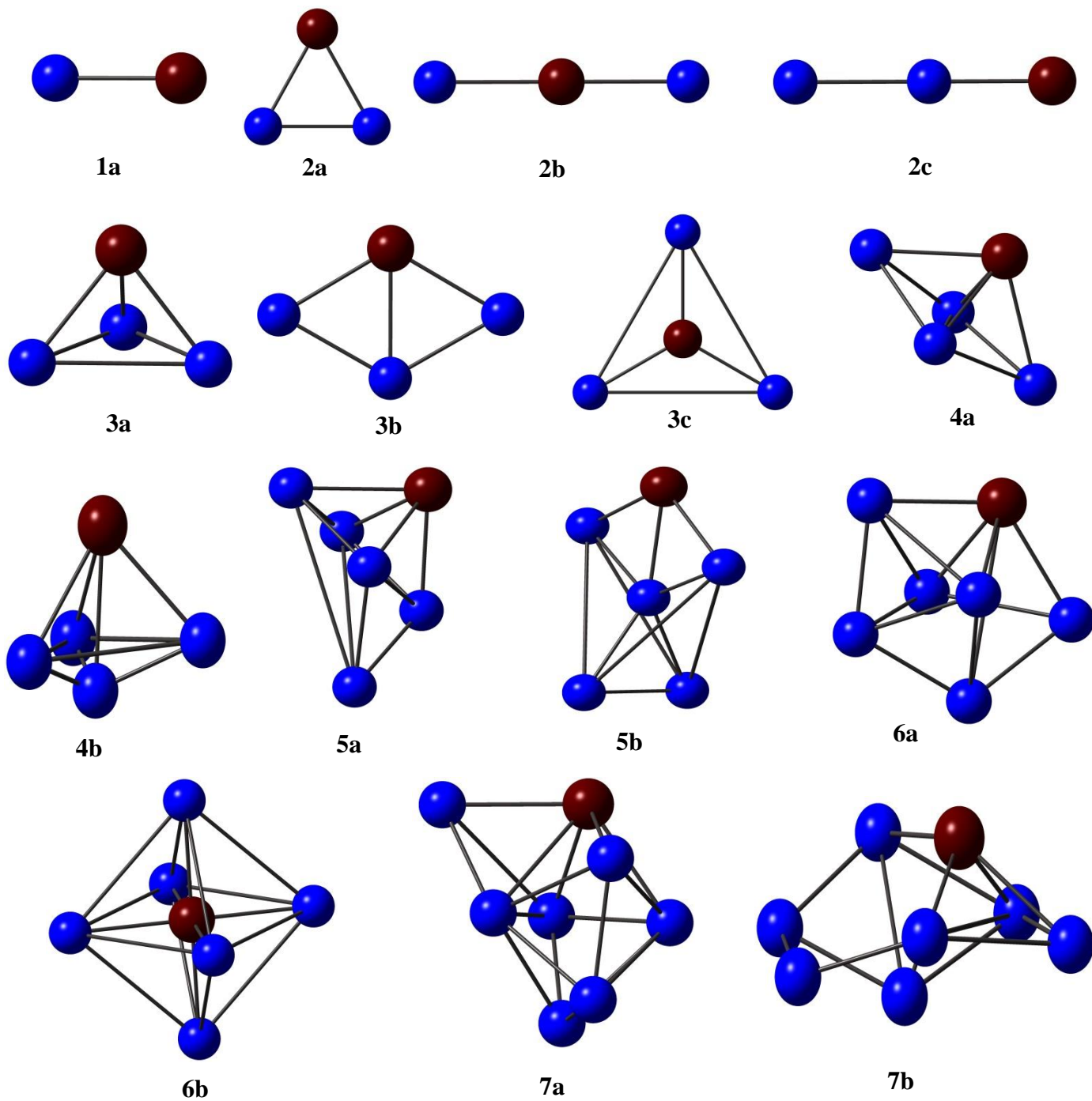


Figure – 2

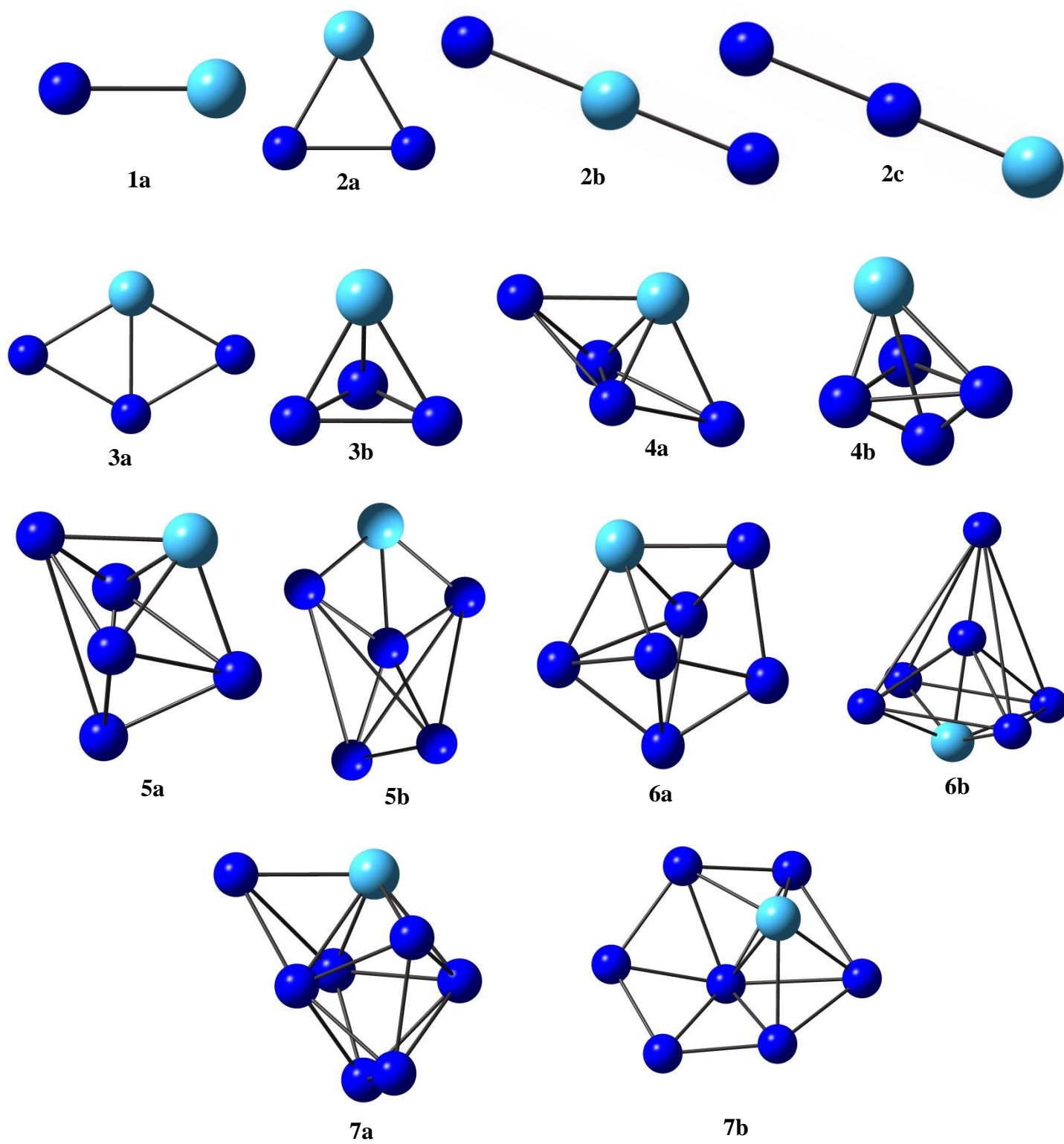


Figure – 3

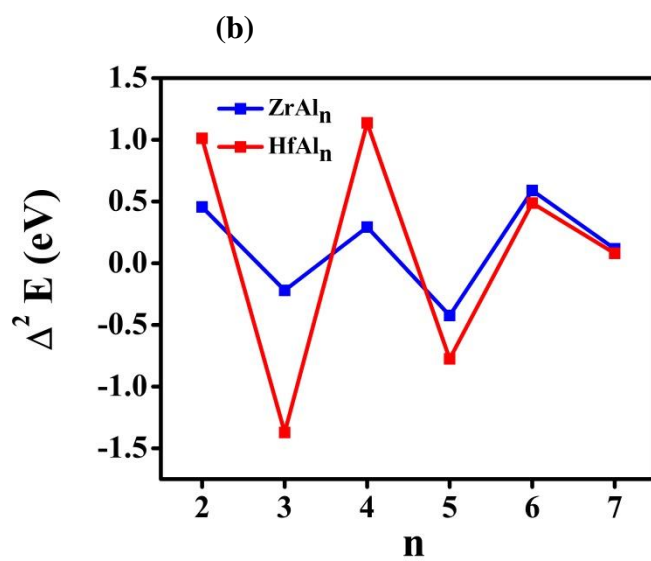
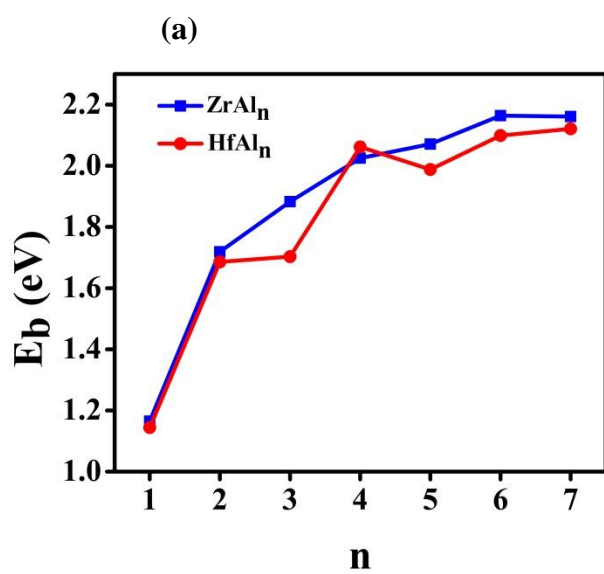


Figure – 4

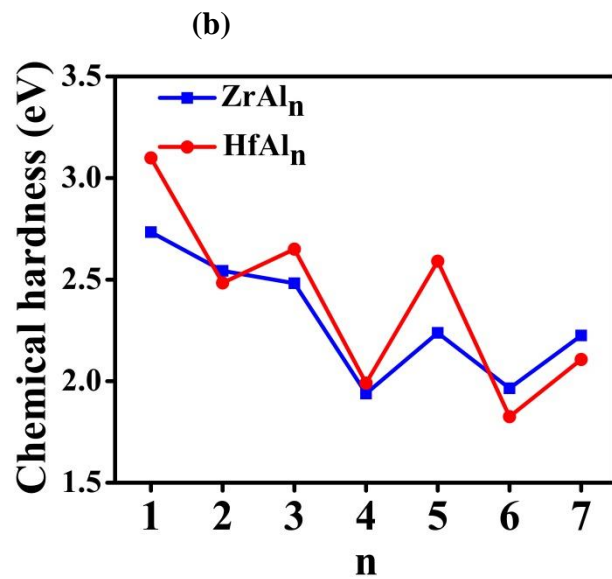
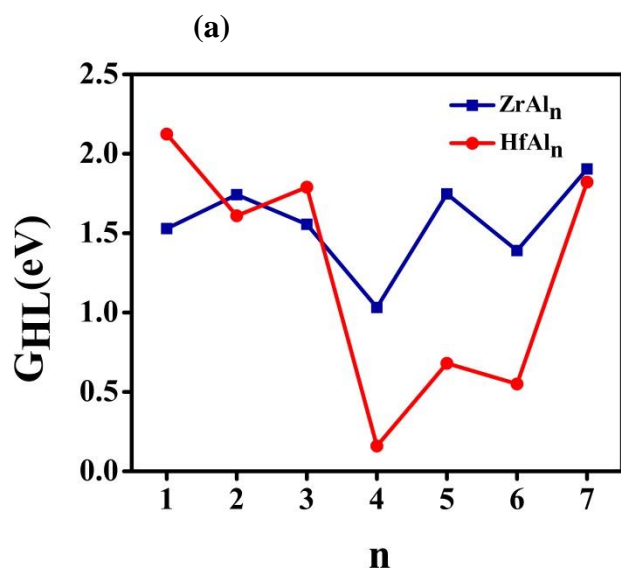


Figure – 5

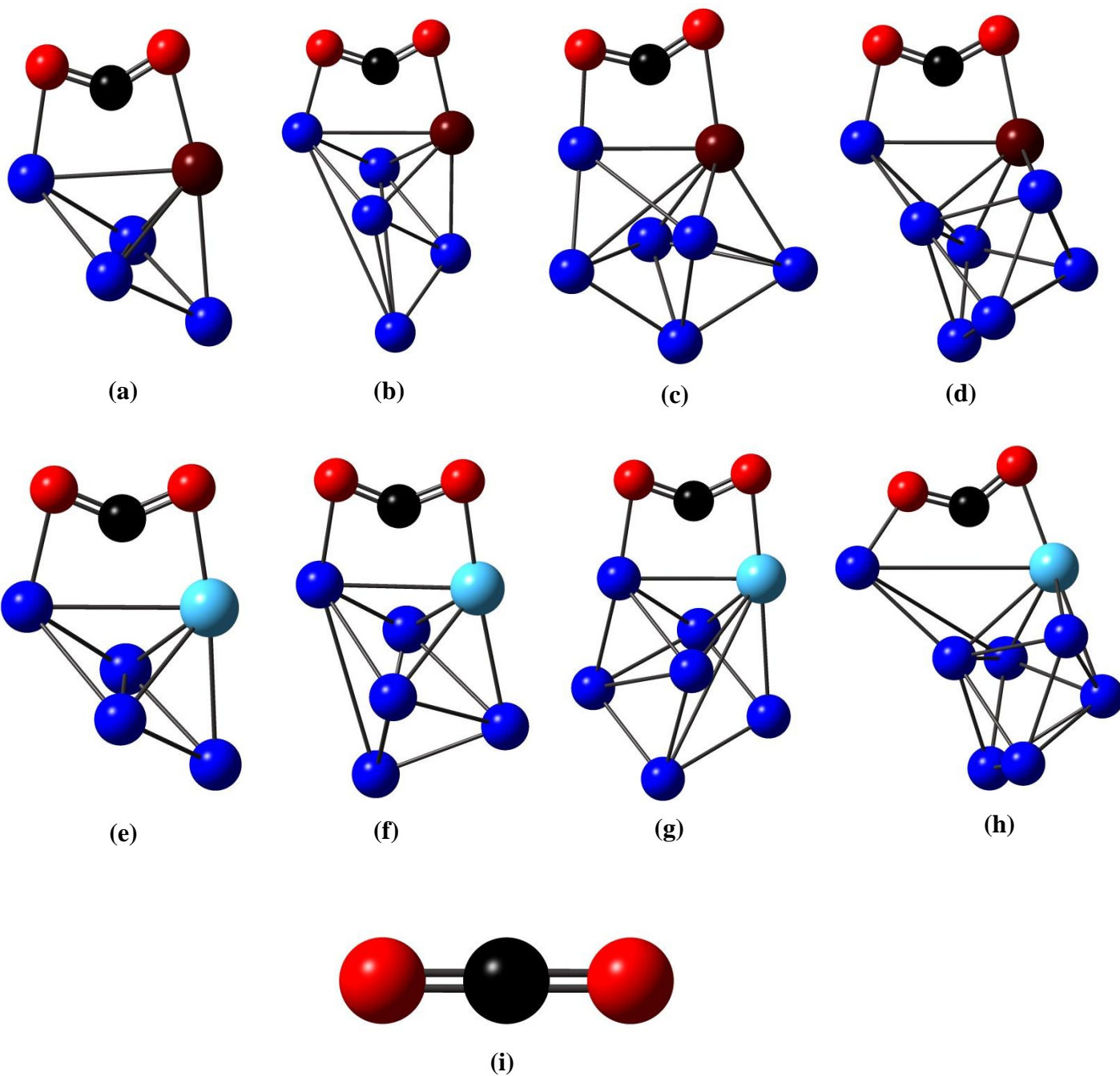


Figure – 6

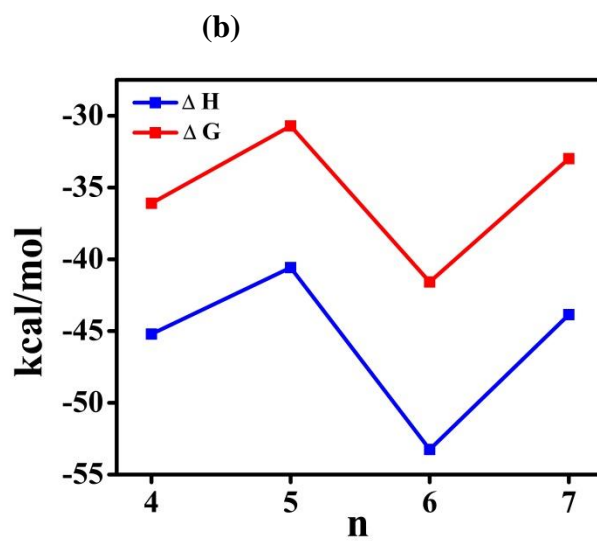
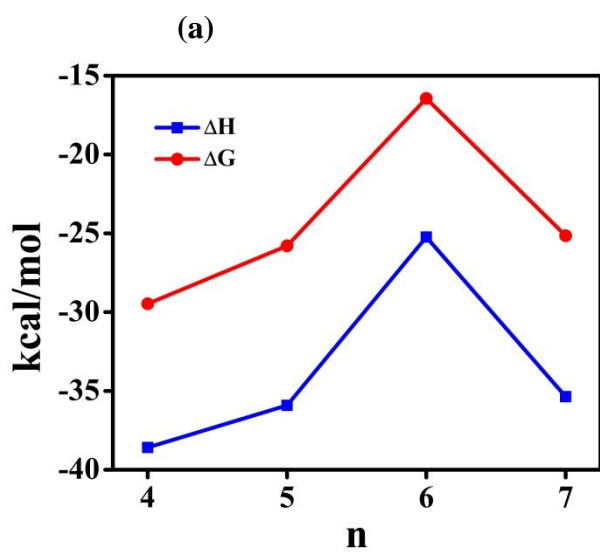


Table – 1: Structural symmetry, binding energy and 2nd order difference in total energy with ionization energy for the ZrAl_n and HfAl_n clusters

Clusters(multiplicity)	Symmetry	E _b (eV)	Δ ² E (eV)	Ionization Energy (eV)
ZrAl	C _{∞v}	1.165	---	6.565
ZrAl ₂	C _s	1.719	0.456	6.293
ZrAl ₃	C _s	1.883	-0.220	6.501
ZrAl ₄	C _{2v}	2.025	0.293	5.931
ZrAl ₅	C ₁	2.071	-0.424	6.060
ZrAl ₆	C _{2v}	2.164	0.589	6.049
ZrAl ₇	C ₁	2.161	0.117	6.494
HfAl	C _{∞v}	1.144	---	7.157
HfAl ₂	C _{2v}	1.686	1.012	6.402
HfAl ₃	C _s	1.703	-1.372	6.833
HfAl ₄	C _{2v}	2.062	1.137	6.032
HfAl ₅	C ₁	1.988	-0.776	6.789
HfAl ₆	C _{2v}	2.099	0.487	6.003
HfAl ₇	C ₁	2.121	0.080	6.256

Table – 2: HOMO-LUMO gap, Atomic charge on Tm and chemical hardness for ZrAl_n and HfAl_n

Clusters	HOMO-LUMO gap (eV)	Atomic charge (a.u.)	Chemical hardness (eV)
ZrAl	1.529	-0.090	2.734
ZrAl ₂	1.742	-0.128	2.543
ZrAl ₃	1.555	-0.871	4.965
ZrAl ₄	1.032	-1.061	1.939
ZrAl ₅	1.747	-0.715	2.238
ZrAl ₆	1.391	-1.122	1.965
ZrAl ₇	1.903	-1.324	2.225
HfAl	2.214	-0.073	3.099
HfAl ₂	1.609	-0.182	2.484
HfAl ₃	1.789	-0.945	2.650
HfAl ₄	0.159	-1.345	1.990
HfAl ₅	0.680	-1.095	2.591
HfAl ₆	0.549	-1.002	1.825
HfAl ₇	1.822	-1.223	2.107

Table – 3: Thermochemical data (enthalpy and free energy difference) of adsorption of CO₂ on ZrAl_n and HfAl_n (n = 4 to 7).

Clusters	ΔE (kcal/mol)	ΔH (kcal/mol)	ΔG (kcal/mol)
ZrAl ₄	-39.152	-38.587	-29.465
ZrAl ₅	-35.097	-35.912	-25.796
ZrAl ₆	-25.065	-25.232	-16.443
ZrAl ₇	-35.235	-35.363	-25.148
HfAl ₄	-45.106	-45.215	-36.096
HfAl ₅	-40.467	-40.580	-30.708
HfAl ₆	-53.240	-53.253	-41.580
HfAl ₇	-43.798	-43.855	-32.991